Supplementary Information (SI) for Dalton Transactions.
This journal is © The Royal Society of Chemistry 2025

Supporting Information

Enhanced Electrochemical Performance of NiCo-LDH by Inner Sulfur Doping Design

Chemicals and materials

Concentrate hydrochloric acid (HCl) was purchased from Sinopharm Chemical Reagent Co., Ltd. Nickel nitrate hexahydrate ($Ni(NO_3)_2·6H_2O$, AR) was purchased from Shanghai Wokai Biotechnology Co., Ltd. Cobalt nitrate hexahydrate ($Co(NO_3)_2·6H_2O$, AR) was bought from Shandong Keyuan Biochemical Co., Ltd. Thiourea ($SC(NH_2)_2$, AR) was purchased from Shenyang Xinhua Reagent Factory. Potassium hydroxide (KOH, AR) was purchased from Tianjin Damao Chemical Reagent Factory. Anhydrous ethanol (C_2H_5OH) was bought from Tianjin Fuyu Fine Chemical Co., Ltd. The flexible activated carbon electrode was purchased from Shijiazhuang Aokezhuo Instrument Technology Co., Ltd. All above chemical reagents were used directly without further purification. Nickel foam (1 cm×3 cm , Suzhou Chint New Materials Co., Ltd.) was ultrasonicated in 3 M HCl for 30 min to remove surface oxides and other impurities. Then it was washed several times with anhydrous ethanol and deionized water and vacuum dried at 60 ℃ for 12 h for later use.

The gravimetric specific capacitance (C_m, F g^{-1}), and specific capacity (C_{sc}, mAh g^{-1}) were calculated using the following formulas:

$$C_m = \frac{I \times \Delta t}{m \times \Delta V} \qquad \text{(S1)}$$

$$C_{SC} = \frac{I \times \Delta t}{3.6 \times S} \qquad \text{(S2)}$$

Where I is the discharge current (A), Δt is the discharge time (s), ΔV is the potential window during the discharge process (V) and m is the mass loading of the active material (g).

The gravimetric specific capacitance (C_m, F g^{-1}), energy density (E, Wh kg^{-1}), and power density (P, W kg^{-1}) were calculated using equations S3-S5.

$$C_m = \frac{I \times \Delta t}{m \times \Delta V} \qquad \text{(S3)}$$

$$E = \frac{C_m \times \Delta V^2}{2 \times 3.6} \qquad \text{(S4)}$$

$$\mathrm{P} = \frac{3600 \times E}{\Delta \mathrm{t}} \qquad \text{(S5)}$$

Where I (A) is the discharge current, m (g) is the mass loading of the active material, ΔV (V) is the potential window of the ASC, and Δt (s) is the discharge time.

The relationship between the peak current (ipeak, A) and the scan rate (v, mV s^{-1}) was calculated, with the dependence expressed by equation S6:

$$\log i_{peak} = b \log v + \log a \quad \text{(S6)}$$

where, i denotes current response, presents scanning rate, a and b represent constants. The charge storage kinetics is controlled by diffusion processes if b is 0.5, while it is surface-controlled process when b-values equal to 1.

The capacitance contribution was calculated with the following equation:

$$i(V) = k_1 v + k_2 v^{1/2} \quad \text{(S7)}$$

Where i(V), v, k_1v, and k_2v represent the current value, scan rate, capacitive process, and diffusion-controlled process, respectively. The k_1 and k_2 values can be obtained by fitting the linear line $i(V)/v^{1/2}$ versus $v^{1/2}$.

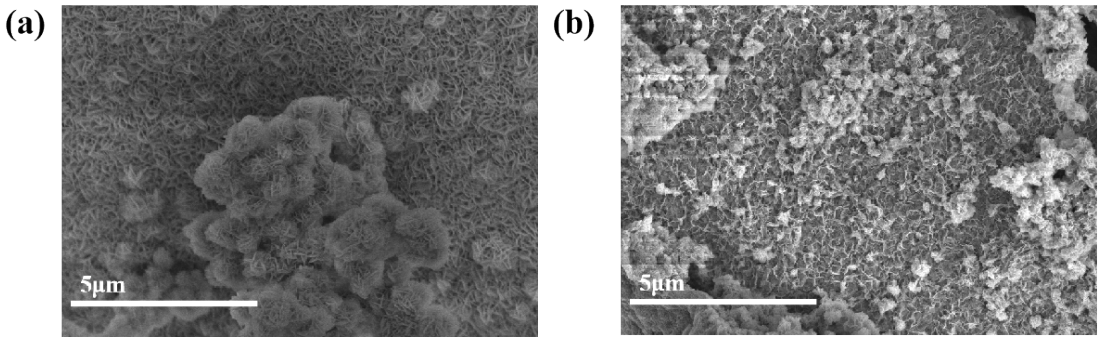

Fig. S1. SEM images of (a) NiCo-LDH/NF; (b) S-NiCo-LDH/NF.

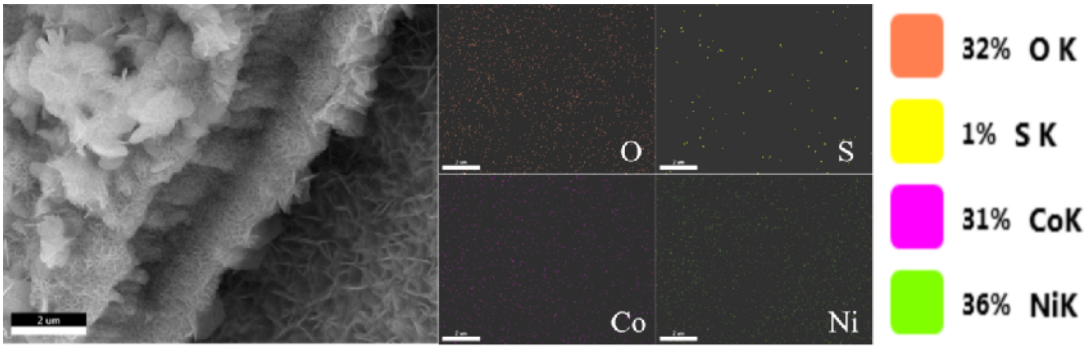

Fig. S2. Elemental mapping images of S-NiCo-LDH@NiCo-LDH/NF.

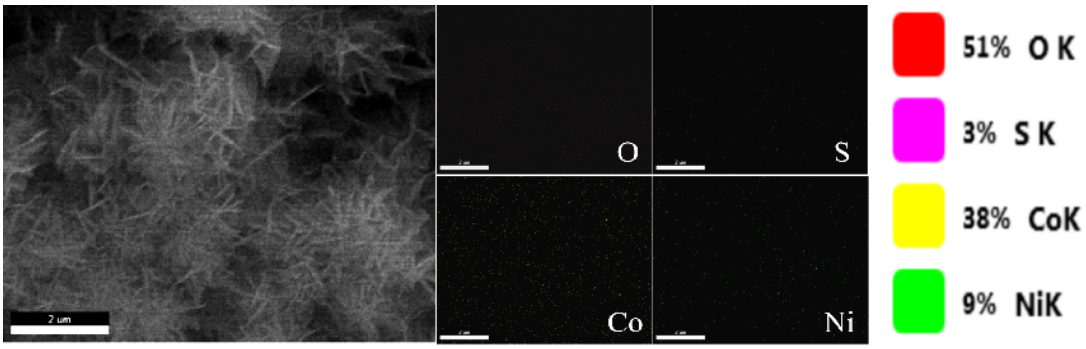

Fig. S3. Elemental mapping images of S-NiCo-LDH/NF.

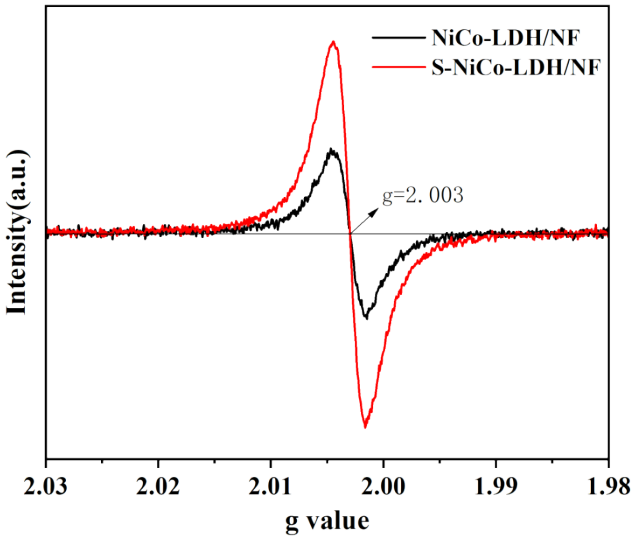

Fig.S4. The EPR images of NiCo-LDH/NF and S-NiCo-LDH/NF.

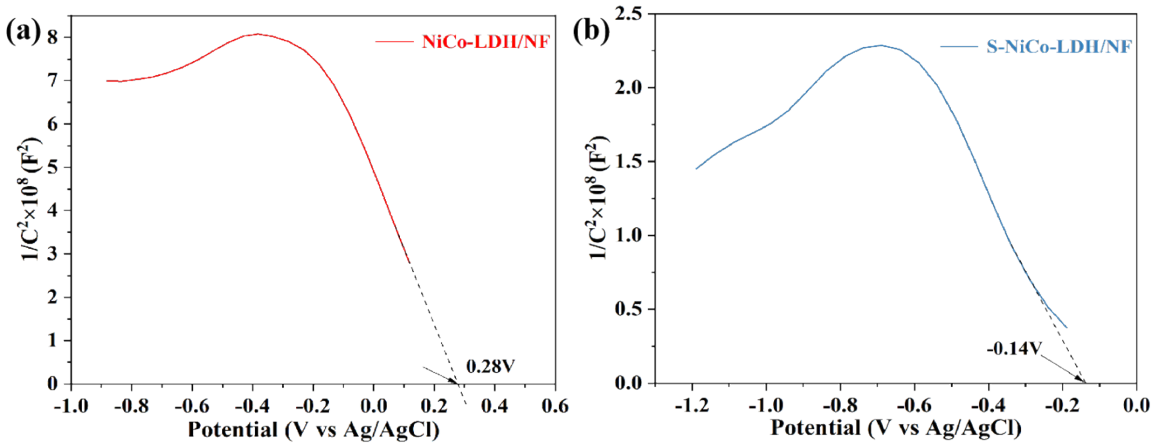

Fig. S5. Mott–Schottky plots of (a) NiCo-LDH/NF; (b) S-NiCo-LDH/NF.

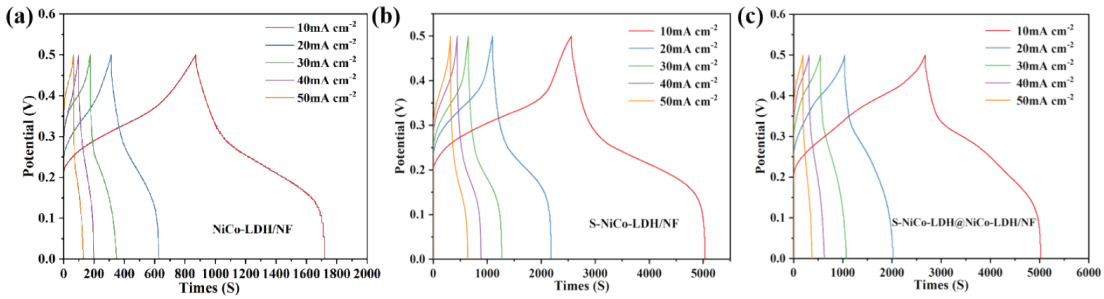

Fig. S6. GCD curves at different current densities. (a) NiCo-LDH/NF; (b) S-NiCo-LDH/NF; (c) S-NiCo-LDH@NiCo-LDH/NF.

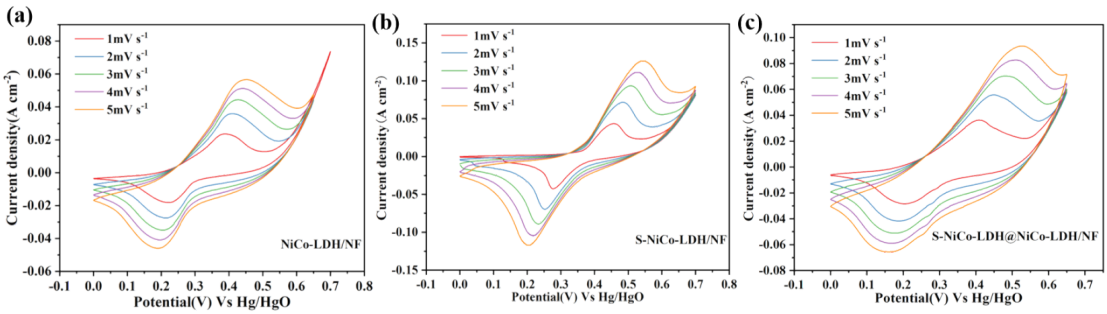

Fig. S7. CV curves at different scan rates. (a) NiCo-LDH/NF; (b) S-NiCo-LDH/NF; (c) S-NiCo-LDH@NiCo-LDH/NF.

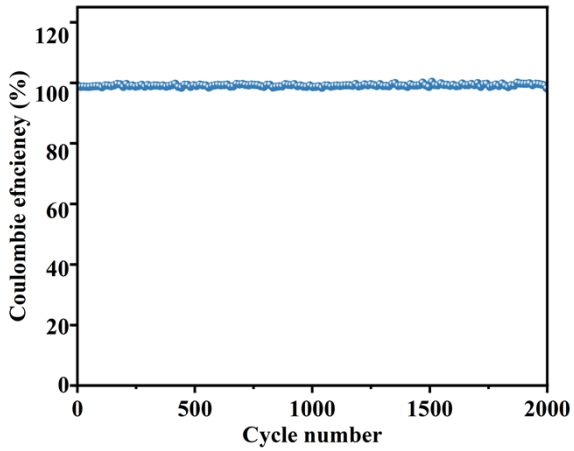

Fig. S8. The Coulombic efficiency of S-NiCo-LDH@NiCo-LDH/NF at 50 mA cm^{-2}.

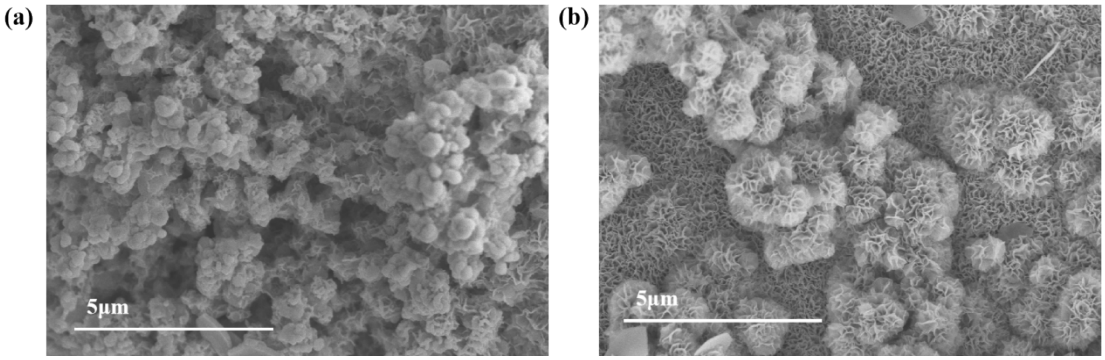

Fig. S9. SEM images after 1000 cycles at a current density of 50 mA cm^{-2}. (a) S-NiCo-LDH/NF; (b) S-NiCo-LDH@NiCo-LDH/NF.

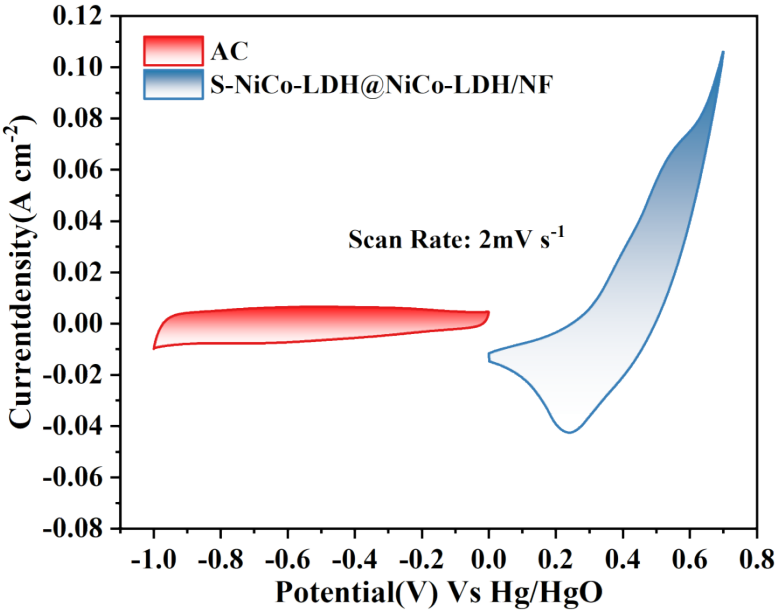

Fig. S10. CV curves of S-NiCo-LDH@NiCo-LDH/NF and AC at 2 mV s^{-1}

Table S1. The calculated crystallinity of prepared LDHs

	Area of the crystalline portion	Area of the amorphous portion	Total area	Crystallinity
NiCo-LDH/NF	11985.665	100825.132	112810.797	10.62%
S-NiCo-LDH/NF	9709.756	136719.128	146428.884	6.63%
S-NiCo-LDH@NiCo-LDH/NF	9401.791	115237.847	124639.638	7.54%

Table S2. The capacitance of NiCo-LDH based materials

Materials	Current density	Specific capacity	KOH concentration	Ref.
S-NiCo-LDH@NiCo-LDH/NF	10 mA cm^{-2}	1473 F g^{-1} (205 mAh g^{-1})	2 M	This work
CC/$NiCo_2O_4$/CoNi-LDH	1 A g^{-1}	893.33 F g^{-1}	3 M	1
NiCo-LDH@PC	1 A g^{-1}	596 F g^{-1}	6 M	2
$Cu(OH)_2$@NiCo-BH	1 mA cm^{-2}	1262 F g^{-1}	3 M	3
NiCo-LDH	1 A g^{-1}	950 F g^{-1}	6 M	4
$NiCoSe_2$@NiCo-LDH@CC	5 mA cm^{-2}	2609.1 mF cm^{-2} (1242.4 F g^{-1})	3 M	5
NiCo-LDH@$Ti_3C_2T_x$	1 A g^{-1}	919.5 F g^{-1}	3 M	6
NiCo-LDH/STSC	1 A g^{-1}	210 F g^{-1}	6 M	7
3D Ni-Co LDH/NiNw	5 mA cm^{-2}	466.6 F g^{-1}	6 M	8

Table S3. The fitted resistance values of prepared samples

Sample	Rs (Ω)	Rct (Ω)
S-NiCo-LDH@NiCo-LDH/NF	**0.97**	**0.10**
S-NiCo-LDH/NF	**1.02**	**0.11**
NiCo-LDH/NF	**1.06**	**0.12**

Table S4. Sulfur element concentration in electrolyte after cycles.

Electrode	1000 cycles	1500 cycles	2000 cycles
S-NiCo-LDH/NF	11.83	16.57	22.49
S-NC-LDH@NC-LDH/NF	10.9	12.22	12.3

Table S5. Metal element concentration in electrolyte after 1000 cycles.

Electrode	Ni(μg/L)	Co(μg/L)
S-NiCo-LDH/NF	5.56	34.49
S-NiCo-LDH@NiCo-LDH/NF	3.52	32.6
reduction（%）	36.7%	5.45%

Reference

1. H. Gao, X. Li and Y. Ma, Journal of Colloid and Interface Science, 2025, 695, 137802.

2. X. Cheng, X. Liu, L. Li, L. Zhang, H. Wu, J. Zheng, J. Li and T. Yi, Journal of Energy Storage, 2025, 129, 117357.

3. X. Leng, L. Zhao, W. Shi, J. Lian and X. Zhang, The Journal of Physical Chemistry C, 2024, 128, 9422-9434.

4. N. Poompiew, P. Pattananuwat and P. Potiyaraj, ACS Omega, 2021, 6, 25138-25150.

5. Y. Jiang, B. Cai, Y. Yang, F. Yu, Y. Sun, X. Qi, L. Wang, X. Li and X. Yang, Journal of Energy Storage, 2022, 56, 106001.

6. Z. Bai, D. Zhang, Y. Guo, Y. Yang, H. Yan, Y. Wang, J. Cheng, P. K. Chu, H. Pang and Y. Luo, Advanced Sustainable Systems, 2021, 6, 2100371.

7. D. Zhang, X. Guo, X. Tong, Y. Chen, M. Duan, J. Shi, C. Jiang, L. Hu, Q. Kong and J. Zhang, Journal of Alloys and Compounds, 2020, 837, 155529.

8. H. Wan, L. Li, Y. Xu, Q. Tan, X. Liu, J. Zhang, H. Wang and H. Wang, Nanotechnology, 2018, 29, 194003.